International Journal of Applied Pharmaceutics

ISSN- 0975-7058 Vol 12, Issue 4, 2020

Original Article

MICROENCAPSULATION OPTIMIZATION OF PROPOLIS ETHANOLIC EXTRACT FROM TETRAGONULA SPP USING RESPONSE SURFACE METHODOLOGY

DIAH KARTIKA PRATAMI[1], ABDUL MUN'IM[2], HERI HERMANSYAH[3], MISRI GOZAN[3, 4], MUHAMAD SAHLAN[3, 4*]

[1]Lab of Pharmacognosy and Phytochemistry, Faculty of Pharmacy, Pancasila University, Jakarta, 12640, Indonesia, [2]Department of Pharmacognosy and Phytochemistry, Faculty of Pharmacy, Universitas Indonesia, Depok, West Java, 16424, Indonesia, [3]Department of Chemical Engineering, Faculty of Engineering, Universitas Indonesia, Depok, West Java, 16424, Indonesia, [4]Research Center for Biomedical Engineering, Faculty of Engineering, Universitas Indonesia, Depok, West Java, 16424, Indonesia
Email: sahlan@che.ui.ac.id

Received: 08 Apr 2020, Revised and Accepted: 01 Jun 2020

ABSTRACT

Objective: This research aimed to encapsulate the propolis through spray drying to overcome problematic handling properties of propolis and to optimize the microencapsulation by using response surface methodology (RSM).

Methods: The propolis ethanolic extract (PEE) was microencapsulated by spray drying with maltodextrin and gum arabic. RSM was applied for the optimization of microencapsulation efficiency, yield, moisture content, solubility in water, total phenolic content (TPC), and antioxidant activity of spray-dried propolis (SDP) microcapsules.

Results: The highest process efficiency reached a microencapsulation yield of 75.35%. The highest solubility of SDP in water was 91.47%, with a moisture content of 0.96%. SDP exhibiting the highest TPC of 307.325 mg GAE/g, with a microencapsulation efficiency of 81.48%. Ferric reducing antioxidant power analysis showed its highest antioxidant activity with a low EC_{50} 19.12 ug/ml with DPPH analysis, and a high reducing power capacity of 314.64 mg GAE/g.

Conclusion: Microencapsulation optimization of propolis ethanolic extract from *Tetragonula spp.* using RSM indicated that SDP with 1:2 ratios of the microwall to core (propolis), inlet temperature at 115 °C, and flow rate 20% represented the optimum conditions. Microencapsulation has successes improved physical appearance and the solubility index and protected and enhanced bioactive compounds and antioxidant properties of propolis in optimum condition by using spray drying.

Keywords: Antioxidant activity, Microencapsulation, Propolis, Response surface methodology, Spray-drying, *Tetragonula spp*

DOI: http://dx.doi.org/10.22159/ijap.2020v12i4.37808. Journal homepage: https://innovareacademics.in/journals/index.php/ijap

INTRODUCTION

Propolis is a primary product produced by bees, besides honey, which is widely used in the health sector [1]. It is a mixture of bee saliva and gum produced by leaf buds and stems generated by plants and collected by bees [2]. It acts as the primary protection for bees' nests [3]. The chemical composition of propolis depends on the geography and plant-dependent variables [4]. Previous research has discovered the existence of various components contained in propolis, such as phenolic acid, caffeic acid phenethyl ester (CAPE), flavonoids, terpenoids, fatty acids, steroids, aromatic aldehydes, and alcohols [5-10]. Tetragonula spp produces more propolis than other bee species because of their stingless and small body sizes [11].

Propolis contains high antioxidant activities. Chemical profiling using UPLC–TOF–MS from our previous study was performed on propolis ethanolic extract (PEE) from Tetragonula spp. The identified chemical components included (-)-sesamin $C_{20}H_{18}O_6$, curcumin $C_{21}H_{20}O_6$, 8-epi-helenalin $C_{15}H_{18}O_4$, and kushenol-F $C_{25}H_{28}O_6$, all of which display antioxidant activities [12]. Therefore, it could be utilized for the development of medicinal, food, and cosmetic or supplement products. The antioxidant potency of propolis is also valuable in the pharmaceutical industry because of its effect on the retardation of lipid oxidation and its enhanced product stability and long shelf life [13].

However, the application of propolis in pharmaceutical drugs is hampered by its characteristics of low water solubility, sticky physical appearance, bitter taste, and aroma [13, 14]. Propolis microencapsulation using the spray drying method could be employed to overcome these problematic obstacles. The protection of bioactive substances and an increase in the dose potency are predicted using a water-soluble encapsulation matrix [15, 16].

Microencapsulation by spray drying can be optimized by combining the Box–Behnken factorial experimental design with RSM, a mathematical model used for the analysis of multiple parameters and their interactions, to reduce the number of experiments [17]. This research aimed to optimize microencapsulation to obtain spray-dried propolis (SDP) and to overcome problematic handling properties of propolis using RSM methods. For this purpose, we investigated the simultaneous influence of inlet temperature, the ratio of active ingredients with an encapsulant, and extract flow rate on microcapsule production in terms of six different responses, namely, total polyphenol content (TPC), microencapsulation yield (MY), moisture content (MC), solubility in water, reducing power capacity, and EC_{50} antioxidant activity.

MATERIALS AND METHODS

Samples

Smooth propolis, taken from inside the nests of Tetragonula spp, were purchased from RIN Biotek Indonesia Company, with origins from Masamba, North of Luwu District, South Sulawesi Province of Indonesia.

Chemicals

Gallic acid, ethanol, and methanol were purchased from Merck Co. (Darmstadt, Germany). 2,2-Diphenyl-1-picrylhydrazyl (DPPH), ferric chloride, 2,4,6-tri(2-pyridyl)-s-triazine (TPTZ), acetic acid (glacial) anhydrous, Folin–Ciocalteu reagent, and pharmaceutical grade sodium carbonate were purchased from Sigma Aldrich Co. (Singapore). Maltodextrin 97 dextrose equivalent (DE) 18 and gum arabic (GA) 98 were obtained from Brataco Co. (Indonesia).

Microencapsulation of propolis by spray drying

PEE was prepared from smooth propolis taken from inside Tetragonula spp beehives using the method described in Sahlan *et al.* (2013) [18]. The coating material was prepared from maltodextrin (MD) and GA as described by Da Silva (2013) and

Andresa Berretta (2015), with some modifications [13, 19]. The ratio between the coating material and propolis was defined by three formulas—F1, F2, and F3—as shown in table 1. The ratio of the formulation of the core material and microwall defined after observation in the preformulation. The coating material MD and GA (10:1) was prepared by stirring 10 g of MD and 1.0 g of GA in 100 ml of distilled water at 6000 rpm for 30 min. It was then homogenized in Ultra-Turrax T18 (IKA, Konigswinter, Germany) at 15,000 rpm for 2 min. The PEE solution (36.067 mg/ml solid) related to ratios F1, F2, or F3 was then gradually added and homogenized in the Ultra-Turrax T18 for an additional 2 min. Spray drying was conducted using a mini spray dryer (Buchi B290, Flawil, Switzerland) in the closed mode in combination with the Inert Loop B-295. Operational conditions of the spray dryer were as follows: aspirator, 100%; spray gas, 600 L/min; nozzle diameter, 1.5 mm; varying feed rate, 20%–30%; and inlet temperature, 100 °C–120 °C.

Table 1: The formulation of microwall and core material as a coating material

Formula	MD/GA: Propolis
F1	1:2
F2	1:1
F3	2:1

MD/GA: Maltodextrin and Gum Arabic

Microencapsulation yield (MY)

The MY was calculated by determining the mass lost during spray drying, as calculated in Equation 1:

$$\text{MY} = \frac{\text{mass of the powdered after drying}}{\text{theoritical mass}} \times 100 \quad (1)$$

Morphology characterization

The morphology of SDP microcapsules was observed under a scanning electron microscope (SEM) in the Central Forensic Laboratory (PUSLABFOR) in Jakarta, Indonesia.

Total phenolic content determination

TPC was determined according to the method of Ahmad *et al.* (2017), with some modifications [20]. An aliquot of 25 uL of diluted SDP was mixed with 100 uL of 1:4 diluted Folin–Ciocalteu reagent in a flat-bottom 96-well microplate and incubated for 4 min. The mixture was then added to 75 uL of sodium carbonate solution (100 gL^{-1}). After incubation at room temperature for 2 h, absorbance was measured at 765 nm using a microplate reader (VERSAmax; Molecular Devices, USA). Standards used were gallic acid solutions (5–300 mg/l).

Microencapsulation efficiency

Microencapsulation efficiency (% ME), as calculated by equation 2,

$$\%\ \text{ME} = \frac{\text{A} - \text{B}}{\text{A}} \times 100 \quad (2)$$

Where A is total phenolics content (TPC) initially added to the solution entering the spray dryer (mg GAE/g), and B is The TPC unencapsulated in the spray-dried powder (mg GAE/g).

The measurement of the moisture content of SDP

One gram of each SDP microcapsule compound was applied for MC measurement using the moisture balance analyzer AMB (Adam, USA) at 105 °C.

The solubility of SDP in water

Solubility was determined according to the gravimetric analysis method. Solubility (%) was calculated by the weight difference of filter paper using equation 3:

$$\text{Solubility}\ (\%) = \left[1 - \left(\frac{\text{Pc} - \text{Pb}}{\frac{100 - \%\ \text{MC x Pa}}{100}}\right)\right] \text{x}\ 100\ \%\ (3)$$

Where Pc (g) is the mass of the filter paper plus sample after drying, Pb (g) is the initial mass of the filter paper, Pa (g) is the weight of the sample, and MC (%) is the MC of the sample.

Antioxidant assay measurement with DPPH

The antioxidant assay using the DPPH assay was performed as described by Pratami *et al.* (2018) [12]. An aliquot of 20 µl of the diluted sample was added to 180 µl of DPPH solution (150 µmol L^{-1}) in ethanol, shaken for 60 s in a 96-well microplate, and then incubated for 40 min in the dark at room temperature. Absorbance at 515 nm was measured using a microplate reader. The % DPPH quenched was calculated using equation 4:

$$\%\ \text{DPPH quenched} = \left[1 - \left(\frac{\text{Asample} - \text{Ablank}}{\text{Acontrol} - \text{Ablank}}\right)\right] \text{x}\ 100 \quad (4)$$

Where Asample is the absorbance of extract or standard; Ablank is the absorbance of 200 µl ethanol, and Acontrol is the absorbance of ethanol with DPPH solution (20:180 µl). All calculations were performed in triplicate. The concentration of samples resulting in 50% inhibition of DPPH (EC50 value, ug/ml) was calculated using Microsoft Office Excel or Softmax Pro 6.

Measurement of reducing power capacity

The measurement was based on Ferric Reducing Antioxidant Power (FRAP) assay described by Bolanos De La Torre (2014) and DK Pratami (2018) with some modifications [12, 21]. The FRAP reagent solution contains 10:1:1 of acetate buffer (300 mmol, pH 3.6), TPTZ (40 mmol dissolved with 40 mmol HCl), and ferric chloride (20 mmol in water). The procedure of the FRAP method assay is displayed in table 2. Absorbance was measured at 595 nm using a microplate reader. The standard for the calibration curve was calculated using gallic acid at 5–500 µmol L^{-1}. The FRAP reducing power capacity was expressed as mg GAE/g and calculated using the equation of linear regression using Microsoft Office Excel and Soft Max Pro6.5.1 software.

Experimental design

Microencapsulation experiments were performed according to a factorial Box–Behnken design using 3^k (three-level factorial design). Response surface methodology (RSM) with Design-Expert® Software Version 10 (Stat-Ease, Inc., Minneapolis, USA) the three independent variables, namely, inlet temperature (T, °C), formulation core: microwall ratio (F, Propolis: MD/GA), and sample feed rate (FR, %), with a total of 17 experiments (table 3). MY, TPC, MC, solubility in water (SW), DPPH, and FRAP represent the six responses, all of which were completed in triplicate and analyzed using statistical ANOVA analysis for the significance of the model and 3D graphical optimization.

Table 2: **FRAP assay procedure**

	Material	Volume (µl)	
	Blank	Control blank	Positive control/sample
FRAP reagent	-	270	270
Standard/Sample	-	-	30
Ethanol p. a	300	30	-

Incubated for a half-hour at 37 °C and measured absorbance with a *microplate reader* at λ 595 nm

Table 3: **Three-level factorial design experiment with box behnken**

Run	X_1	X_2	X_3	T (°C)	The formulation	Flow rate (%)
1	-1	0	-1	100	F2	20
2	1	0	-1	120	F2	20
3	-1	0	1	100	F2	30
4	1	0	1	120	F2	30
5	-1	1	0	100	F3	25
6	1	-1	0	120	F1	25
7	-1	1	0	100	F3	25
8	1	1	0	120	F3	25
9	0	-1	-1	110	F1	20
10	0	-1	1	110	F1	30
11	0	1	-1	110	F3	20
12	0	1	1	110	F3	30
13	0	0	0	110	F2	25
14	0	0	0	110	F2	25
15	0	0	0	110	F2	25
16	0	0	0	110	F2	25
17	0	0	0	110	F2	25

RESULTS AND DISCUSSION

Experimental design optimization of microencapsulation

The experimental Box–Behnken design was used to predict the optimized condition of the microencapsulation process. Table 4 lists the coded values of the independent variables used in the factorial Box–Behnken design, including inlet temperature (T, °C), formulation core: microwall ratio (F, Propolis: MD/GA), and sample flow rate to the spray dryer (FR, %), as well as the experimental variables of the responses, namely, MY (%), TPC (mg GAE/g), MC (%), SW (%), EC50 DPPH (ug/ml), and FRAP capacity (FRAP, mg GAE/g).

The experimental values of responses listed in table 4 analyzed with statistical analysis ANOVA to obtain the polynomial equation to demonstrate the significant effect of independent variables on the independent variable. Mathematical models were obtained for each response, whose coefficients, after elimination of the statistically no significant terms, are listed in table 5.

Table 4: Responses according the Box Behnken experimental design

Run	MY (%) (Y_1)	TPC (mg GAE/g) (Y_2)	MC (%) (Y_3)	SW (%) (Y_4)	EC_{50} DPPH (µg/ml) (Y_5)	FRAP (mg GAE/g) (Y_6)
1	38.98+1.65	264.85+2.30	0.96+0.05	73.74+1.35	54.34	311.24+11.95
2	45.89+3.56	230.75+4.63	1.47+0.02	77.99+0.42	29.10	279.57+29.42
3	66.91+4.40	64.55+5.28	7.35+0.35	89.79+0.96	178.02	45.00+2.51
4	72.75+2.65	91.10+13.54	6.37+0.05	86.00+1.50	38.63	134.44+10.09
5	62.02+3.74	105.67+6.47	6.18+0.15	85.81+1.74	112.84	72.23+12.84
6	69.81+1.56	181.31+1.29	6.90+1.48	85.50+1.41	85.60	83.53+0.73
7	68.82+2.65	93.65+2.94	5.85+0.05	85.21+1.47	86.10	70.00+4.04
8	75.35+3.16	142.02+3.31	6.17+1.22	86.36+1.29	86.32	91.57+1.46
9	51.71+2.25	307.33+4.52	4.34+0.16	85.45+2.30	19.12	224.12+13.84
10	69.53+3.15	75.60+5.41	6.95+1.21	91.47+1.35	161.32	51.45+1.20
11	39.78+1.76	270.02+3.70	0.98+0.03	75.26+1.26	30.88	314.64+14.72
12	71.59+1.58	110.73+14.57	6.42+0.76	79.33+1.17	37.45	142.25+20.39
13	68.77+1.76	156.07+3.35	5.73+0.84	88.22+1.35	107.97	71.56+4.54
14	67.67+2.65	169.20+2.04	7.03+1.28	87.82+1.25	116.54	81.83+1.75
15	64.98+0.59	130.41+0.29	6.19+1.26	85.32+0.48	119.73	82.26+2.91
16	65.63+3.25	193.94+3.41	6.61+1.58	86.57+0.96	114.25	81.83+4.45
17	66.33+2.65	149.68+2.53	6.63+1.56	85.18+1.21	122.02	83.02+4.49

Note. MY: microencapsulation yield, TPC: total phenolic content, GAE: gallic acid equivalents, TF, ME: microencapsulation efficiency, MC: moisture content, SW: solubility in water, EC_{50} DPPH: effective concentration 50% antioxidant capacity with DPPH assays, FRAP: Reducing power capacity with FRAP assays. The experiment results are the mean value±SD of three replicates.

Table 5: Mathematical equation from a model for each response

Coefficient	MY (%)	TPC (mg GAE/g)	MC (%)	SW (%)	EC_{50} DPPH (µg/ml)	FRAP (mg GAE/g)
X_0	66.91	160.91	6.44	84,31	116.10	80.10
X_1	3.38	14.56	0.071	0.16	-23.96	-11.33
X_2	13.05	-91.37	2.42	4.21	35.25	-94.55
X_3	-1.39	-6.68	-0.62	-2.77	-10.58	-23.39
X_{12}	0.27	0	-0.37	0	-28.54	30.28
X_{13}	3.08	0	-0.10	0	-6.51	2.57
X_{23}	3.50	0	0.71	0	-33.91	0.069
X_1^2	0.038	0	-0.40	0	-5.28	4.34
X_2^2	-10.81	0	-2.00	0	-35.08	108.13
X_3^2	2.06	0	0.24	0	-18.11	-5.11

Note: The coefficient: X_1=inlet temperature; $X_{2=}$ ratio (mwall: mcore); X_3=flow rate

Table 6: Results of ANOVA for MY, TPC, MC, SW, EC_{50} DPPH, and FRAP

Response	Source	SS	DF	MS	F-Value	p-value	R^2
MY (%)	Model	2059.44	9	228.83	72.86	<0.0001	0.9894
	Residual	21.99	7	3.14			
	Lack of fit	12.92	3	4.31	1.90	0.2708	
	Pure Error	9.06	4	2.27			
	Total	2081.42	16				
TPC	Model	68840.63	3	22946.88	20.26	<0.0001	0.8238
(mg GAE/g)	Residual	14724.90	13	1132.68			
	Lack of fit	12490.37	9	1387.82	2.48	0.1976	
	Pure Error	2234.53	4	558.63			
	Total	83565.53	16				
MC (%)	Model	70.44	9	7.83	15.31	0.0008	0.9517
	Residual	3.58	7	0.51			
	Lack of fit	2.60	3	0.87	3.54	0.1269	
	Pure Error	0.98	4	0.24			
	Total	74.01	16				
SW (%)	Model	203.44	3	67.81	4.90	0.0172	0.5305
	Residual	180.03	13	13.85			
	Lack of fit	172.11	9	19.12	9.66	0.0216	
	Pure Error	7.92	4	1.98			
	Total	383.47	16				
EC_{50} DPPH	Model	30825.95	9	3425.11	4.84	0.0247	
(µg/ml)	Residual	4950.24	7	707.18			
	Lack of fit	4832.30	3	1610.77	54.63	0.0011	
	Pure Error	117.94	4	29.48			
	Total	35776.19	16				
FRAP	Model	130300.00	9	14474.90	22.17	0.0002	0.9661
(mg GAE/g)	Residual	4569.96	7	652.85			
	Lack of fit	4477.88	3	1492.63	64.84	0.0008	
	Pure Error	92.07	4	23.02			
	Total	134869.96	16				

The ANOVA analysis obtained from the independent variables (X_1, X_2, dan X_3) and the microencapsulation yields (Y_1) of SDP produced a polynomial equation as follows:

$$Y_1 = 66.91+3.38X_1+13.05X_2-1.39X_3-0.27X_1X_2+3.08X_1X_3+3.50X_2X_3+$$

$$0.038X_1^2-10.81X_2^2+2.06X_3^2 \ldots\ldots (5)$$

The statistical analysis from Equation 5 shows a good quadratic model with R-squared = 0,9894 (R-squared>0.7), which means the equation model can be used to predict the optimum condition. Adj. R-squared = 0.9759 and Pred. R-squared = 0.8939, which means that it is within the acceptable criteria. The Adj-squared>0.8 represent that the polynomial equation provides a good model where the difference of Adj.-squared from the pred. R-squared less than 0.2.

The response variable MY demonstrated the model was significant with ($p<0.05$), the model could illustrate a significant effect of inlet temperature, ratio microwall: core, and flow rate on the response variable MY of the three factors. Inlet temperature exhibited the strongest effect on the MY, although ratio microwall: core and flow rate also showed some effects. Fig. 1 illustrates the tridimensional plots of MY obtained by RSM using the above model.

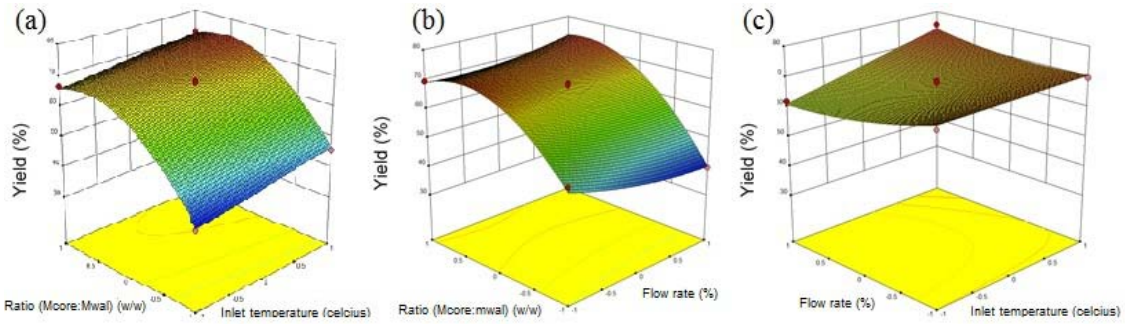

Fig. 1: 3D model tridimensional plots of the microencapsulation yield responses obtained by RSM. (a) Microencapsulation yields versus ratio (core: microwall) and inlet temperature; (b) Microencapsulation yields versus ratio (core: microwall) and flow rate; (c) Microencapsulation yields versus flow rate and inlet temperature

The ANOVA analysis obtained from the independent variables (X_1, X_2, dan X_3) and the total polyphenol content (Y_2) of SDP produced a polynomial equation as follows:

$$Y_2 = 160.99+14.56X_1-91.37X_2-6.68X_3 \quad (6)$$

The statistical analysis from Equation 6 shows a good linear model with R-squared = 0.8238 (R-squared>0.7), which means the equation model can be used to predict the optimum condition. Adj. R-squared = 0.7831 and Pred. R-squared = 0.6570. Which means that it is within the acceptable criteria. The polynomial equation provides a good model where the difference of Adj.-squared from the pred. R-squared less than 0.2. The response variable TPC demonstrated the model could illustrate a significant effect of ratio microwall: core, but a not significant effect of inlet temperature and flow rate on the response variable TPC. Fig. 2 illustrates the tridimensional plots of TPC obtained by RSM using the above model.

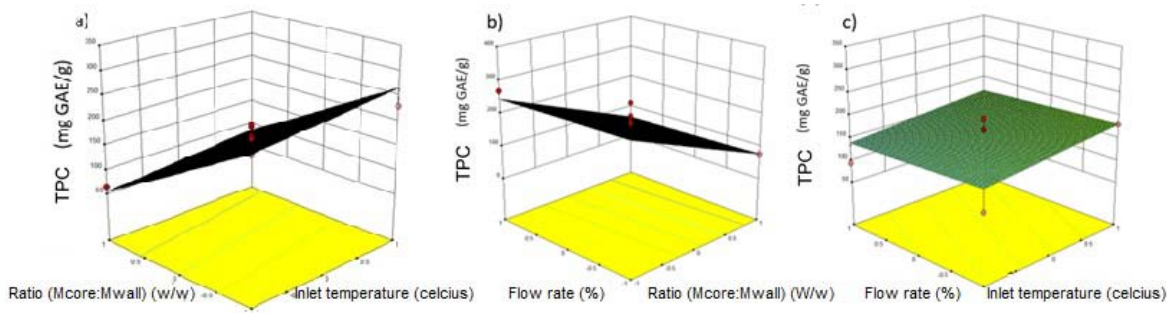

Fig. 2: 3D model tridimensional plots of total polyphenol content responses obtained by RSM. (a) Total polyphenol content versus ratio (core: microwall) and inlet temperature; (b) Total polyphenol content versus ratio (core: microwall) and flow rate; (c) Total polyphenol content versus flow rate and inlet temperature

The ANOVA analysis obtained from the independent variables (X_1, X_2, dan X_3) and the moisture content (Y_3) of SDP produced a polynomial equation as follows:

$$Y_3 = 6.44+0.071X_1+2.42X_2-0.62X_3-0.37X_1X_2-0.10X_1X_3+0.71X_2X_3-0.4X_1^2-2X_2^2+0.24X_3^2 \ldots\ldots (7)$$

The statistical analysis from Equation 7 shows a good quadratic model with R-squared = 0.9517 (R-squared>0.7), which means the equation model can be used to predict the optimum condition. Adj. R-squared = 0.8895 and Pred. R-squared = 0.4177, the difference of Adj.-squared from the pred. R-squared more than 0.2, means there was a significant effect between factors and the observed response, although it did not satisfy the criteria as a good model. The response variable MC demonstrated the model was significant with ($p<0.05$), the model could illustrate a significant effect of ratio microwall: core and flow rate, but no significant effect of inlet temperature on the response variable MC of the three factors. Fig. 3 illustrates the tridimensional plots of MC obtained by RSM using the above model.

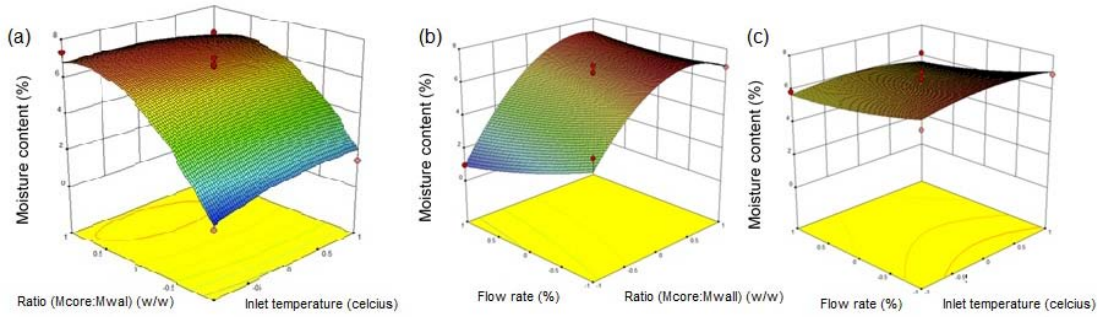

Fig. 3: 3D model tridimensional plots of moisture content responses obtained by RSM. (a) Moisture content versus ratio (core: microwall) and inlet temperature; (b) Moisture content versus ratio (core: microwall) and flow rate; (c) Moisture content versus flow rate and inlet temperature

The ANOVA analysis obtained from the independent variables (X_1, X_2, dan X_3) and the solubility in water (Y_4) of SDP produced a polynomial equation as follows:

$$Y_4 = 84.31+0.16X_1+4.21X_2-2.77X_3 \ldots\ldots (8)$$

The statistical analysis from Equation 8 shows a good linear model with R-squared = 0.5305 (R-squared<0.7), which means the equation model cannot be used to predict the optimum condition. Adj. R-squared = 0.4222 and Pred. R-squared = 0.0982. Which means that it is not the acceptable criteria. The polynomial equation does not provide a good model where the difference of Adj.-squared from the pred. R-squared more than 0.2. The response variable SW demonstrated the model could illustrate a significant effect of ratio microwall: core and flow rate, but a not significant effect of inlet temperature on the response variable SW. Fig. 4 illustrates the tridimensional plots of SW obtained by RSM using the above model.

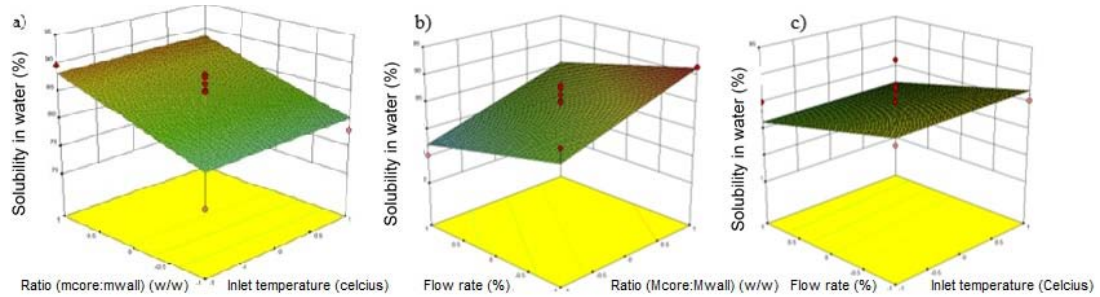

Fig. 4: 3D model tridimensional plots of solubility in water responses obtained by RSM (a) SW versus ratio (core: microwall) and inlet temperature; (b) SW versus ratio (core: microwall) and flow rate; (c) SW versus flow rate and inlet temperature

The ANOVA analysis obtained from the independent variables (X_1, X_2, dan X_3) and the EC50 DPPH (Y_5) of SDP produced a polynomial equation as follows:

$$Y_5 = 116.1 - 23.96X_1 + 35.25X_2 - 10.58X_3 - 28.54X_1X_2 - 6.51X_1X_3 - 33.91X_2X_3 - 5.28X_1^2 - 35.8X_2^2 - 18.11X_3^2 \quad \ldots\ldots (9)$$

The statistical analysis from Equation 9 shows a good quadratic model with R-squared = 0.8616 (R-squared>0.7), which means the equation model can be used to predict the optimum condition. Adj. R-squared = 0.8837 and Pred. R-squared = 0.8663, which means that it is within the acceptance criteria that the polynomial equation provides a good model.

The response variable EC50 DPPH demonstrated the model was significant with ($p<0.05$), the model could illustrate a significant effect of ratio microwall: core and inlet temperature, but no significant effect of flow rate on the response variable EC50 DPPH of the three factors. Fig. 5 illustrates tridimensional plots of EC50 DPPH obtained by RSM using the above model.

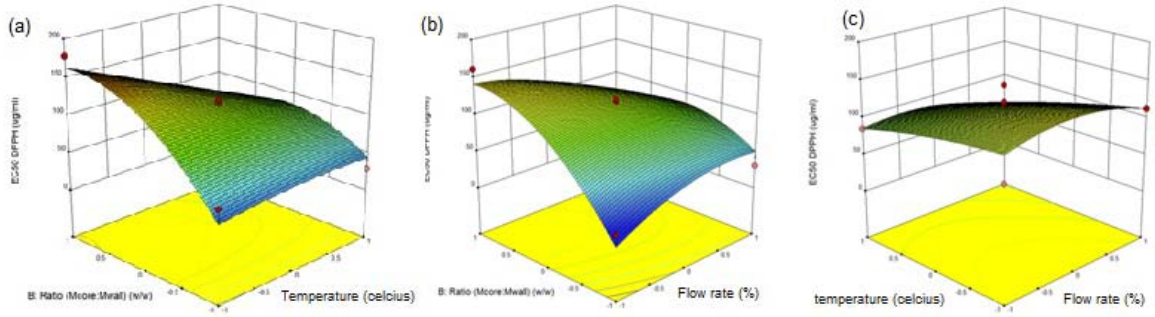

Fig. 5: 3D model tridimensional plots of EC_{50} DPPH responses obtained by RSM. (a) EC_{50} DPPH versus ratio (core: microwall) and inlet temperature; (b) EC_{50} DPPH versus ratio (core: microwall) and flow rate; (c) EC_{50} DPPH versus flow rate and inlet temperature

The ANOVA analysis obtained from the independent variables (X_1, X_2, dan X_3) and the FRAP reducing capacity (Y_6) of SDP produced a polynomial equation as follows:

$$Y_5 = 80.1 - 11.33X_1 - 94.55X_2 - 23.39X_3 + 30.28X_1X_2 + 2.57X_1X_3 + 0.069X_2X_3 + 4.34X_1^2 + 108.13X_2^2 - 5.11X_3^2 \quad \ldots\ldots\ldots (9)$$

The statistical analysis from Equation 9 shows a good quadratic model with R-squared = 0.8616 (R-squared>0.7), which means the equation model can be used to predict the optimum condition. Adj. R-squared = 0.9225 and Pred. R-squared = 0.9676, which means that it is within the acceptance criteria that the polynomial equation provides a good model.

The response variable FRAP reducing capacity demonstrated the model was significant with ($p<0.05$), the model could illustrate a significant effect of ratio microwall: core and flow rate, but no significant effect of inlet temperature on the response variable FRAP reducing the capacity of the three factors. Fig. 6 illustrates tridimensional plots of FRAP reducing capacity obtained by RSM using the above model.

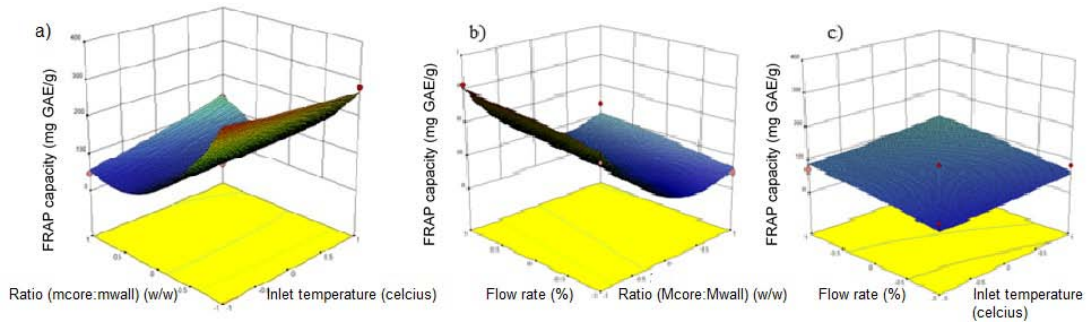

Fig. 6: 3D model tridimensional plots of FRAP reducing capacity responses obtained by RSM. (a) FRAP reducing capacity versus ratio (core: microwall) and inlet temperature; (b) FRAP reducing capacity versus ratio (core: microwall) and flow rate; (c) FRAP reducing capacity versus flow rate and inlet temperature

Table 7: The criteria of factors and responses to determine the optimum microencapsulation

Name	Goal	Lower limit	Upper limit	Importance
A: T (°C)	is in range	100	120	3
B: Formulation	is in range	0.5	2	3
C: Flow Rate (%)	is in range	20	30	3
MY	Maximize	38.98	75.35	5
TPC	Maximize	64.55	307.32	4
MC	is in range	0.96	7.35	3
SW	Maximize	73.72	91.02	4
EC_{50} DPPH	Minimize	19.12	178.02	3
FRAP capacity	Maximize	45.00	314.64	3

Note: 5= most important; 4= important; 3= middle important; 2= less important; and 1= not important

The Design Expert 12.0 software can predict the optimum microencapsulation based on the six equations above with selected criteria (presented in table 7). The optimum microencapsulation obtained from the Design Expert 11.0 software can be seen in fig. 7. The predicted optimum condition was comprised of inlet temperature at 114.9 °C, F1 (microwall: mcore=1:2), and the flow rate of 20.15 %. At optimal conditions, the highest level of desirability of 0.724 was achieved. The excellent fit with an R^2 = 0.9991 for the experimental results of an additional test conducted under these optimal conditions compared with that expected by numerical optimization suggested that the factorial design had an excellent reproducibility.

Solutions

53 Solutions found

Number	Inlet temperature	Formulation	Flow rate	Microencapsulation Yields	TPC	MC	SW	EC50 DPPH	FRAP capacity	Desirability	
1	**114.901**	**0.500**	**20.148**	**51.973**	**305.607**	**3.585**	**82.241**	**13.103**	**243.429**	**0.724**	**Selected**
2	114.940	0.500	20.186	52.372	304.366	3.624	82.235	13.753	241.979	0.724	
3	114.921	0.500	20.108	51.577	307.295	3.526	82.206	12.095	245.743	0.724	
4	114.755	0.500	20.126	51.692	305.569	3.595	82.324	13.370	242.710	0.724	
5	115.051	0.500	20.128	51.828	307.309	3.518	82.132	11.870	246.362	0.724	
6	115.234	0.500	20.250	53.108	303.667	3.629	82.081	13.665	242.405	0.724	
7	114.480	0.500	20.037	50.663	307.319	3.553	82.461	12.829	243.726	0.724	
8	114.329	0.500	20.012	50.333	307.330	3.561	82.549	13.083	243.035	0.724	
9	115.340	0.500	20.366	54.277	299.815	3.752	82.081	15.710	237.799	0.724	
10	115.204	0.500	20.414	54.702	297.188	3.850	82.194	17.447	233.724	0.724	
11	115.686	0.500	20.226	52.989	307.330	3.475	81.777	10.813	249.329	0.724	
12	114.678	0.500	20.363	54.025	296.006	3.922	82.495	19.014	229.825	0.724	
13	114.921	0.500	20.419	54.660	295.340	3.930	82.372	18.984	230.035	0.724	
14	114.877	0.500	20.471	55.143	293.141	4.006	82.427	20.323	226.956	0.723	
15	116.324	0.500	20.741	57.969	291.110	3.977	81.723	19.119	230.592	0.722	
16	113.948	0.500	20.276	52.817	294.868	4.003	82.916	20.937	225.086	0.722	
17	116.717	0.500	20.674	57.368	295.775	3.791	81.444	15.831	238.559	0.721	
18	115.807	0.500	20.778	58.253	286.937	4.153	82.050	22.337	222.815	0.719	
19	117.967	0.500	20.924	59.427	292.661	3.796	80.922	15.750	239.835	0.717	
20	119.160	0.500	20.709	57.080	307.319	3.192	80.030	5.691	265.313	0.709	

Fig. 7: The optimum condition of microencapsulation predicted by design expert

Microencapsulation yield (MY)

In particular, fig. 1 shows that MY varied between 38.98% and 75.35% and reached its maximum value at the high temperature of 120 °C, displayed a maximum flow rate of 30%, and an intermediate core: microwall ratio of 1:1. The MY was directly proportional to the inlet temperature, flow rate, and core: microwall ratio. The maximum value of this response was higher than that reported for microencapsulation with MD of Satureja montana extract (60%) [22], Salvia fruticose Miller extract (60%) [23], and soy sauce powder (62.4%) [24]. SDP microcapsules have a better spray drying yield value than microparticles propolis proposed by Andresa Baretta (2015), with the encapsulating agent GA and silicon dioxide (1:1) resulting in yields between 31.85% and 67.60% [19].

Total polyphenol content (TPC)

Fig. 2 shows that TPC varied between 64.5547 and 307.325 mg GAE/g and reached its maximum value at the intermediate temperature of 110 °C, minimum microwall: core ratio was 2:1, and the minimum flow rate was 30%. These values were higher than those obtained by Kuck and Norena (2016) (25.03 mg GAE/g) for a Vitis lambrusca using MD and GA as the microencapsulating agent [25]. TPC was directly proportional to the microwall: core ratio but not significantly influenced by inlet temperature and flow rate (table 5). The great variability of TPC may depend on the fact that the encapsulation efficiency is largely dependent on (a) the core: wall ratio, (b) its concentration, i.e., the ratio of dispersed to continuous phase, (c) interaction between active compound and polymer, and (d) solubility of the former in the continuous phase [26, 27].

The total phenolics encapsulated in the microcapsule can be expressed by the value of the total phenolic ME. The value of ME can be determined by comparing the total amount of phenolic analysis with the theoretical content. The ME value ranged from 11.85% to 81.48%; the ME value of SDP microcapsules in this study is similar to a study conducted by Da Silva *et al.* (2013) [13]. Microparticles with propolis: microwall ratio of 1:6 have an ME ranging from 85.1%±0.9%, whereas microparticles with propolis: microwall ratio of 1:4 coatings have an impressive efficiency rating of 76%±1% [13]. In a study conducted by Onbas Rabia (2016), microencapsulation of propolis extracts with complex simultaneous conservation obtained an ME close to 100%, with the highest efficiency value reaching 98.77% [28].

Greater ratios of microwall increase the value of ME. Higher levels of encapsulant used will increase the capability of the encapsulating propolis to form microcapsules. The ME value of efficient microencapsulation can be achieved when a maximum number of core materials can be encapsulated within microcapsules. The ME value is also influenced by the speed of the drying process and the formation of the coating layer [27].

Moisture content (MC*)* of SDP

Table 5 shows that the MC of SDP ranged between 0.96% and 7.35%. The variability of these results may be due to interactions influencing the moisture of the final product, such as the inlet temperature, microwall: core ratio, and polymer concentration [23]. These contents were higher than those reported for microencapsulation with MD of barberry anthocyanin, 3.07%–4.27% [26]; Salvia fruticosa Miller extract, 3%–4% [23]; gac powders equaling 4.06%–4.87%) [29]; and Rubus spp powder, 1.74% [30].

The measurement of MC below 10% indicates a high percentage of the core material and microwall in the spray-dried powder. MC value should be minimized to prevent decomposition due to microbial contamination or chemical changes [31]. Unencapsulated propolis has low MC due to lipophilic characteristics. The microcapsules F1, which contain high propolis: microwall ratio, have low MC. The microcapsules F2 and F3, which contain lower propolis: microwall ratio, have higher MC due to the hygroscopic characteristic of maltodextrin.

The p-value ANOVA test in table 6 indicates that the MC of SDP was directly proportional to temperature. The inlet and outlet temperatures of spray dryer affect MC of dried propolis. The smaller the inlet temperature, the lower the evaporation rate, so that microcapsules can form with a high membrane density, high water content, low fluidity, and a tendency to form agglomerates. However, if the inlet temperature is too high, then it will lead to excessive evaporation, resulting in the cracking of the coating membrane, induction of core material release, and degradation or evaporation of the core material [32].

Solubility in water (SW)

In this study, SDP showed a higher SW, with values ranging between 73.74% and 91.47%. The highest water dispersibility of SDP was achieved by Suzzana Alvez (2017), where propolis was encapsulated with MD (without added gum) and totaled 97%±3%; propolis with maltodextrin–vinal gum was 100%±1%, and propolis with maltodextrin–GA was 100%±3 230% [14]. Fig. 4 shows that SW was directly proportional to the microwall: core ratio, thereby confirming the observations of effects of different drying conditions and amounts of MD addition during spray drying of sumac extract [33].

EC50 value with DPPH antioxidant assay

Fig. 5 shows that the EC50 value ranged between 19.12 and 178.02 ug/ml and reached its maximum value at the intermediate temperature, with the lowest microwall: core ratio and the lowest flow rate. The EC50 in this study was lower than the antioxidant activity of SDP microcapsules in the study conducted by Souza et al. (2007), who reported a 50% percent inhibition of lipid oxidation with values ranging from 2.5 to 5 mg/ml [34]. The best value of antioxidant activity obtained in the present study was higher than that of the propolis microcapsules obtained by Busch et al. (2017), with EC50 values of 86+9 mg GAE/g (encapsulated with maltodextrin), 81+8 mg GAE/g (encapsulated with maltodextrin–vinyl gum), and 84+9 mg GAE/g (encapsulated with maltodextrin–GA) [14]. Busch et al. showed that the addition of GA can maintain the inhibitory ability of DPPH radicals [14]. This work is related to the research conducted by Da Silva et al. indicated that the addition of GA resulted in higher retention for DPPH free radical absorption [13].

The EC_{50} value is directly proportional to the microwall: core ratio, temperature, and flow rate. An opposite dependence of antioxidant activity on temperature was observed by Silva *et al.* (2013) in their attempt to optimize microencapsulation of Myrciaria jabuticaba extracts using three microwall systems, namely, MD only, MD with GA, and MD with Capsul® [13].

Reducing power capacity value with FRAP assays

Fig. 6 shows that FRAP-reducing power capacity ranged between 45.027 and 314.64 mg GAE/g and reached its maximum value at an intermediate temperature and flow rate, with the lowest microwall: core ratio. The FRAP-reducing power capacity in this study was comparable to that in the study by Busch *et al.*, which produced propolis microcapsules obtained at 10.7+0.6 mmol $FeSO_4$/g (using MD coating) [14]. However, the reduction capacity increased after the addition of vinyl gum and GA as an encapsulation wall material with values of 12.5+0.8 mmol $FeSO_4$/g and 14.7+0.7 mmol $FeSO_4$/g, respectively. The addition of GA to MD can maintain the antioxidant activity of propolis [14].

Morphology characterization of SDP microcapsules

Morphologies of propolis and microparticles were analyzed under SEM (fig. 8). Analyses were conducted at room temperature, and all samples were coated with a layer of gold in a vacuum before microscopy. Micrographs of propolis unencapsulated powder in fig. 8a-b represents agglomerate particles with a non-uniform shape, uneven surfaces, and a diameter ranging from 3 to 9 µm. The SEM image analysis in fig. 8c-d of pure MD-GA powder as microwall shows uniform spherical particles, with sizes ranging from 1 to 8 µm. SDP microcapsules in fig. 8e-f exhibit uniform spherical particles similar to micrographic MD-GA, with sizes ranging from 0.8 to 4 µm. The result of the SEM test showed that the formed SDP microcapsules did not alter the morphology of MD-GA, which indicated the success of microencapsulation because the form of microwall MD-GA was also in uniform spherical matrices. The micrograph of MD-GA powder as an empty microwall with no core material presented curved surfaces and vacuole in its core. The micrograph of SDP microcapsules in which the MD-GA microwall coating the propolis presented a solid spherical microcapsule without a curved surface, thus it can be seen that the propolis has been well encapsulated.

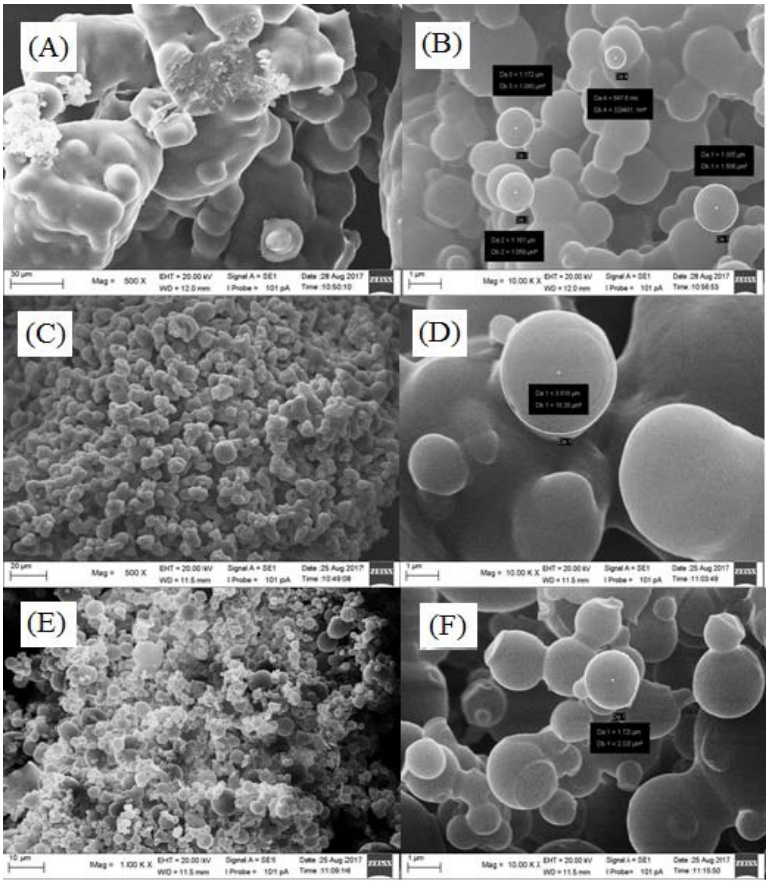

Fig. 8: SEM Image of spray-dried powder. 2(a-b): Propolis without microencapsulation, 2(c-d): SDP microcapsules, 2(e-f): Maltodextrin and gum arabic

SEM micrographs of unencapsulated propolis presented in this study were similar to the visual and microscopic analysis of Brazilian propolis identified by Machado (2016) [35]. The SEM images showed uneven surfaces covered by layers of extractives and wax. SEM images of SDP microcapsules coated with MD and GA showed visual micrographics similar to those observed by Busch (2017) [14]. The microencapsulation improved the size uniformity and microparticle integrity and also showed better core material protection.

CONCLUSION

Microencapsulation of propolis using MD and GA through spray drying can improve the physical characteristics of propolis, including its physical appearance, and increase its SW (>80%) and can maintain the chemical characteristics of propolis, including the protection of substances, bioactive propolis, and antioxidant activity. The optimum conditions of microencapsulation were obtained in formula F1, with an inlet temperature of 115 °C and a flow rate of 20%. From this study, it is suggested that propolis microcapsules can be used for the pharmaceutical development of drugs, cosmetics, and natural additives.

ACKNOWLEDGMENT

The author gratefully acknowledges the financial support from the Ministry of Research and Technology/National Agency for Research and Innovation, the Republic of Indonesia through PPUPT Grant 2020.

FUNDING

Nil

CONFLICT OF INTERESTS

We have no conflicts of interest.

REFERENCES

1. Bankova V. Chemical diversity of propolis and the problem of standardization. J Ethnopharmacol 2005;100:114–7.
2. Bankova V, Castro S De, Marcucci M. Propolis: recent advances in chemistry and plant origin. Apidologie 2000;31:3–15.
3. Simone Finstrom M, Spivak M. Propolis and bee health: the natural history and significance of resin use by honey bees. Apidologie 2010;41:295–311.
4. Huang S, Zhang CP, Wang K, Li GQ, Hu FL. Recent advances in the chemical composition of propolis. Molecules 2014;19:19610–32.
5. Iqbal M, Fan T, Watson D, Alenezi S, Saleh K, Sahlan M. Preliminary studies : the potential anti-angiogenic activities of two Sulawesi Island (Indonesia) propolis and their chemical characterization. Heliyon 2019;5:e01978.
6. Mahadewi AG, Christina D, Hermansyah H, Wijanarko A, Farida S, Adawiyah R, *et al.* Selection of discrimination marker from various propolis for mapping and identify anti-*Candida albicans* activity. AIP Conf Proc 2018;1933. https://doi.org/10.1063/1.5023939
7. Miyata R, Sahlan M, Ishikawa Y, Hashimoto H, Honda S, Kumazawa S. Propolis components from *Stingless bees* collected on South Sulawesi, Indonesia, and their xanthine oxidase inhibitory activity. J Nat Prod 2019;82:205–10.
8. Sahlan M, Mandala DK, Pratami DK, Adawiyah R, Wijarnako A, Lischer K, *et al.* Exploration of the antifungal potential of Indonesian propolis from *Tetragonula biroi* bee on *Candida sp.* and *Cryptococcus neoformans*. Evergr J 2020;7:118–25.
9. Mahadewi AG, Christina D, Hermansyah H, Wijanarko A, Farida S, Adawiyah R, et al. Selection of discrimination marker from various propolis for mapping and identify anti-Candida albicans activity. In: AIP Conference Proceedings. AIP Publishing; 2018. p. 20005.
10. Rahmi S, Sarwono AT, Soekanto SA. Effect of propolis honey candy consumption on the activity of lactoperoxidase in stimulated saliva. Int J Appl Pharm 2019;11:134–6.
11. Sahlan M, Devina A, Pratami DK, Situmorang H, Farida S, Munim A, *et al.* Anti-inflammatory activity of *Tetragronula species* from Indonesia. Saudi J Biol Sci 2018;26:1531–8.
12. Pratami DK, Mun A, Sundowo A, Sahlan M, Pratami DK, Mun A. Phytochemical profile and antioxidant activity of propolis ethanolic extract from *Tetragonula bee*. Pharmacogn J 2018;10:73–80.
13. Da Silva FC, Da Fonseca CR, De Alencar. Assessment of production efficiency, physicochemical properties and storage stability of spray-dried propolis, a natural food additive, using gum Arabic and OSA starch-based carrier systems. Food Bioprod Process 2013;91:28–36.
14. Busch VM, Pereyra Gonzalez A, Segatin N, Santagapita PR, Poklar Ulrih N, Buera MP. Propolis encapsulation by spray drying: characterization and stability. LWT-Food Sci Technol 2017;75:227–35.
15. Biswal I, Dinda A, Das D, Si S, Chowdary KA. Encapsulation protocol for highly hydrophilic drug using nonbiodegradable polymer. Int J Pharm Pharm Sci 2011;3:256-9.
16. Pratami DK, MunIm A, Yohda M, Hermansyah H, Gozan M, Putri YRP, *et al.* Total phenolic content and antioxidant activity of spray-dried microcapsules propolis from *Tetragonula species*. AIP Conf Proc 2019;2085. https://doi.org/10.1063/1.5095018
17. LeClair DA, Cranston ED, Xing Z, Thompson MR. Optimization of spray drying conditions for yield, particle size and biological activity of thermally stable viral vectors. Pharm Res 2016;33:2763–76.
18. Sahlan M, Supardi T. Encapsulation of Indonesian propolis by casein micelle. Int J Pharma Bio Sci 2013;4:297–305.
19. Marquiafavel FS, Nascimento AP, Barud H da S, Marquele Oliveira F, De-Freitas LAP, Bastos JK, *et al.* Development and characterization of a novel standardized propolis dry extract obtained by factorial design with high artepillin C content. J Pharm Technol Drug Res 2015;4:1.
20. Ahmad I, Yanuar A, Mulia K, Munim A. Optimization of ionic liquid-based microwave-assisted extraction of polyphenolic content from *Peperomia pellucida* (L) Kunth using response surface methodology. Asian Pac J Trop Biomed 2017;7:660–5.
21. Bolanos De La Torre AAS, Henderson T, Nigam PS, Owusu Apenten RK. A universally calibrated microplate ferric reducing antioxidant power (FRAP) assay for foods and applications to Manuka honey. Food Chem 2015;174:119–23.
22. Vidovic SS, Vladic JZ, Vastag ZG, Zekovic ZP, Popovic LM. Maltodextrin as a carrier of health benefit compounds in Satureja montana dry powder extract obtained by spray drying technique. Powder Technol 2014;258:209–15.
23. Sahin Nadeem H, Dinçer C, Torun M, Topuz A, Ozdemir F. Influence of inlet air temperature and carrier material on the production of instant soluble sage (*Salvia fruticosa* Miller) by spray drying. LWT-Food Sci Technol 2013;52:31–8.
24. Wang W, Dufour C, Zhou W. Impacts of spray-drying conditions on the physicochemical properties of soy sauce powders using maltodextrin as auxiliary drying carrier. CYTA J Food 2015;13:548–55.
25. Kuck LS, Norena CPZ. Microencapsulation of grape (*Vitis labrusca* var. Bordo) skin phenolic extract using gum Arabic, polydextrose, and partially hydrolyzed guar gum as encapsulating agents. Food Chem 2016;194:569–76.
26. Akhavan Mahdavi S, Jafari SM, Assadpoor E, Dehnad D. Microencapsulation optimization of natural anthocyanins with maltodextrin, gum Arabic and gelatin. Int J Biol Macromol 2016;85:379–85.
27. Jyothi NVN, Prasanna PM, Sakarkar SN, Prabha KS, Ramaiah PS, Srawan GY. Microencapsulation techniques, factors influencing encapsulation efficiency. J Microencapsul 2010;27:187–97.
28. Onbas R, Kazan A, Nalbantsoy A, Yesil Celiktas O. Cytotoxic and nitric oxide inhibition activities of propolis extract along with microencapsulation by complex coacervation. Plant Foods Hum Nutr 2016;71:286–93.
29. Kha TC, Nguyen MH, Roach PD, Stathopoulos CE. Microencapsulation of Gac oil: optimisation of spray drying conditions using response surface methodology. Powder Technol 2014;264:298–309.
30. Caroline FC, Marconi GSP, Dutra AI, Zaratini VF, Maurício de AJ. Influence of carrier agents on the physicochemical properties of blackberry powder produced by spray drying. Int J Food Sci Technol 2012;47:1237–45.
31. Surini S, Azzahrah FU, Ramadon D. Microencapsulation of grape seed oil (*Vitis vinifera* L.) with gum arabic as a coating polymer

by crosslinking emulsification method. Int J Appl Pharm 2018;10:194–8.

32. Gharsallaoui A, Chambin O. Applications of spray-drying in microencapsulation of food ingredients: an overview. Food Res Int 2007;40:1107–21.
33. Caliskan G, Nur Dirim S. The effects of the different drying conditions and the amounts of maltodextrin addition during spray drying of sumac extract. Food Bioprod Process 2013;91:539–48.
34. Souza JPB, Tacon LA, Correia CC, Bastos JK, Freitas LAP. Spray-dried propolis extract, II: Prenylated components of green propolis. Pharmazie 2007;62:488–92.
35. Machado BAS, Silva RPD, Barreto GDA, Costa SS, Da Silva DF, Brandão HN, *et al.* Chemical composition and biological activity of extracts obtained by supercritical extraction and ethanolic extraction of brown, green and red propolis derived from different geographic regions in Brazil. PLoS One 2016;11:1–26.